

## Supporting Information

### Enhanced Emission Efficiency in Doped CsPbBr<sub>3</sub> Perovskite Nanocrystals: The Role of Ion Valence

Mengyu Guan<sup>1, #</sup>, Yunlong Xie<sup>2, #</sup>, Yupeng Wang<sup>1</sup>, Zhuojie He<sup>1</sup>, Lei Qiu<sup>1</sup>, Jun Liu<sup>1</sup>, Keqiang Chen<sup>1</sup>, Shaojiu Yan<sup>1</sup>, Guogang Li<sup>1</sup>, Zhigao Dai<sup>1\*</sup>

<sup>1</sup>Faculty of Materials Science and Chemistry, China University of Geosciences, Wuhan, Hubei 430074, P. R. China.

<sup>2</sup>Institute for Advanced Materials, Hubei Normal University, Huangshi 435002, China

<sup>#</sup>The authors contribute equally to this work.

<sup>\*</sup>To whom correspondence should be addressed. Emails: daizhigao@cug.edu.cn.

- **Detailed method for the calculation of the average lifetime, radiative and nonradiative decay rates:**
- **Table S1.** The change of X-ray diffraction angle corresponding to (110) and (200) crystal planes in Sr<sup>2+</sup>-doped CsPbBr<sub>3</sub> NCs with different Sr<sup>2+</sup> concentrations.
- **Table S2.** The Cs:Pb:Br:Sr/La feed ratio and determined ratio by EDS in undoped and doped samples.
- **Table S3.** The Br/Pb, Br/(Pb+Sr) and Br/(Pb+La) ratios in CsPbBr<sub>3</sub>, Sr<sup>2+</sup>-doped CsPbBr<sub>3</sub> NCs and La<sup>3+</sup>-doped CsPbBr<sub>3</sub> NCs.
- **Table S4.** PLQYs,  $\tau_{ave}$ ,  $k_r$  and  $k_{nr}$  of CsPbBr<sub>3</sub> and Sr<sup>2+</sup>/La<sup>3+</sup>-doped CsPbBr<sub>3</sub> NCs with different doping concentrations.
- **Figure S1.** The XRD pattern of orthorhombic phase CsPbBr<sub>3</sub>.
- **Figure S2.** The size distribution statistics of CsPbBr<sub>3</sub> NCs, Sr<sup>2+</sup>-doped CsPbBr<sub>3</sub> NCs (1.50% Sr<sup>2+</sup>) and La<sup>3+</sup>-doped CsPbBr<sub>3</sub> NCs (1.86% La<sup>3+</sup>)
- **Figure S3.** The UV-vis absorption spectra and (b) the position of absorption peak and PL peak of Sr<sup>2+</sup>-doped CsPbBr<sub>3</sub> NCs with different Sr<sup>2+</sup> concentrations.
- **Figure S4.** The UV-vis absorption spectra of La<sup>3+</sup>-doped CsPbBr<sub>3</sub> NCs with different La<sup>3+</sup> concentrations.
- **Figure S5.** The excitation spectra of CsPbBr<sub>3</sub>, CsPbBr<sub>3</sub>:Sr<sup>2+</sup> and CsPbBr<sub>3</sub>:La<sup>3+</sup>.
- **Figure S6.** The PL spectra of Zn<sup>2+</sup> doped CsPbBr<sub>3</sub> and Al<sup>3+</sup> doped CsPbBr<sub>3</sub>.

**Detailed method for the calculation of the average lifetime, radiative and nonradiative decay rates:** To explore the kinetic luminescence process, we calculated the radiative rate ( $k_r$ ) of perovskite NCs and its non-radiative decay rate ( $k_{nr}$ ) by photoluminescence quantum yield (PLQY) and the average lifetime ( $\tau_{ave}$ ) of the samples. The PLQY is the ratio of the number of photons emitted to the number absorbed. Both the radiative recombination and the non-radiative recombination depopulated the excited state. Hence, the PLQY is also defined as the ratio of the radiative recombination rate to the total recombination rate, given by

$$PLQY = \frac{k_r}{k_r + k_{nr}} \quad (I)$$

The lifetime of the excited state is defined by the average time photon spends in the excited state prior to return to the ground state. The average lifetime is the inverse of the total recombination rate, given by

$$\tau_{ave} = \frac{1}{k_r + k_{nr}} \quad (II)$$

where  $\tau_{avg}$  is the average time calculated by the fitted date of the time-resolved PL decay.

The average lifetime ( $\tau_{avg}$ ) was calculated as follows:

$$\tau_{avg} = \frac{A_1\tau_1^2 + A_2\tau_2^2 + A_3\tau_3^2 + \dots}{A_1\tau_1 + A_2\tau_2 + A_3\tau_3 + \dots} \quad (III)$$

in which  $A_1, A_2, A_3, \dots$  are the amplitudes of each of a series of components and  $\tau_1, \tau_2, \tau_3, \dots$  are the corresponding lifetime constants.

Therefore, we can calculate the radiative and non-radiative recombination rates:

$$k_r = \frac{PLQY}{\tau_{ave}} \quad (IV)$$

$$k_{nr} = \frac{1}{\tau_{ave}} - k_r = \frac{1 - PLQY}{\tau_{ave}} \quad (V)$$

**Table S1.** The change of X-ray diffraction angle corresponding to (110) and (200) crystal planes in Sr<sup>2+</sup>-doped CsPbBr<sub>3</sub> NCs with different Sr<sup>2+</sup> concentrations.

Sample	(110)	(200)
CPB	22.94°	30.55°
CPB:0.30%Sr <sup>2+</sup>	22.96°	30.62°
CPB: 0.69%Sr <sup>2+</sup>	23.01°	30.65°
CPB:0.97%Sr <sup>2+</sup>	23.03°	30.65°
CPB:1.12%Sr <sup>2+</sup>	23.09°	30.66°
CPB:1.50%Sr <sup>2+</sup>	23.10°	30.66°
CPB:1.76%Sr <sup>2+</sup>	23.12°	30.75°

**Table S2.** The Cs:Pb:Sr/La:Br feed ratio and determined ratio by EDS and XPS in undoped and doped samples.

Sample	Feed ratio	Determined ratio by EDS	Determined ratio by XPS
CsPbBr <sub>3</sub>	Cs:Pb:Br = 1:4:8	Cs:Pb:Br = 1:1.1:3.2	Cs:Pb:Br = 1:0.8:2.2
CsPbBr <sub>3</sub> :Sr <sup>2+</sup>	Cs:Pb:Sr:Br = 1:2:2:8	Cs:Pb:Sr:Br = 1:0.9:0.08:3.1	Cs:Pb:Sr:Br = 1:1.1:0.05:3.6
CsPbBr <sub>3</sub> :La <sup>3+</sup>	Cs:Pb:La:Br = 1:2.4:1.1:9.6	Cs:Pb:La:Br = 1:0.9:0.09:3.4	Cs:Pb:La:Br = 1:0.8:0.06:3.3

**Table S3.** The Br/Pb, Br/(Pb+Sr) and Br/(Pb+La) ratios in CsPbBr<sub>3</sub>, Sr<sup>2+</sup>-doped CsPbBr<sub>3</sub> NCs and La<sup>3+</sup>-doped CsPbBr<sub>3</sub> NCs.

Sample	Determined ratio by EDS	Determined ratio by XPS
CsPbBr <sub>3</sub>	Br/Pb = 2.91	Br/Pb = 2.75
CsPbBr <sub>3</sub> :Sr <sup>2+</sup>	Br/(Pb+Sr) = 3.16	Br/(Pb+Sr) = 3.13
CsPbBr <sub>3</sub> :La <sup>3+</sup>	Br/(Pb+La) = 3.43	Br/(Pb+La) = 3.84

**Table S3.** PLQYs,  $\tau_{ave}$ ,  $k_r$  and  $k_{nr}$  of CsPbBr<sub>3</sub> and Sr<sup>2+</sup>/La<sup>3+</sup>-doped CsPbBr<sub>3</sub> NCs with different doping concentrations.

Sample	PLQY (%)	$\tau_{avg}$ (ns)	$k_r$ (ns <sup>-1</sup> )	$k_{nr}$ (ns <sup>-1</sup> )
CPB	55	19	0.0289	0.0237
CPB:0.30%Sr <sup>2+</sup>	65	22	0.0295	0.0159
CPB: 0.69%Sr <sup>2+</sup>	67	23	0.0291	0.0143
CPB:0.97%Sr <sup>2+</sup>	72	24	0.0300	0.0117
CPB:1.12%Sr <sup>2+</sup>	79	25	0.0320	0.0080
CPB:1.50%Sr <sup>2+</sup>	87	26	0.0335	0.0050
CPB:1.76%Sr <sup>2+</sup>	76	23	0.0330	0.0104
CPB:0.57%La <sup>3+</sup>	58	20	0.0290	0.0210
CPB:1.24%La <sup>3+</sup>	70	21	0.0333	0.0143
CPB:1.86%La <sup>3+</sup>	87	26	0.0334	0.0050
CPB:2.43%La <sup>3+</sup>	76	24	0.0316	0.0100

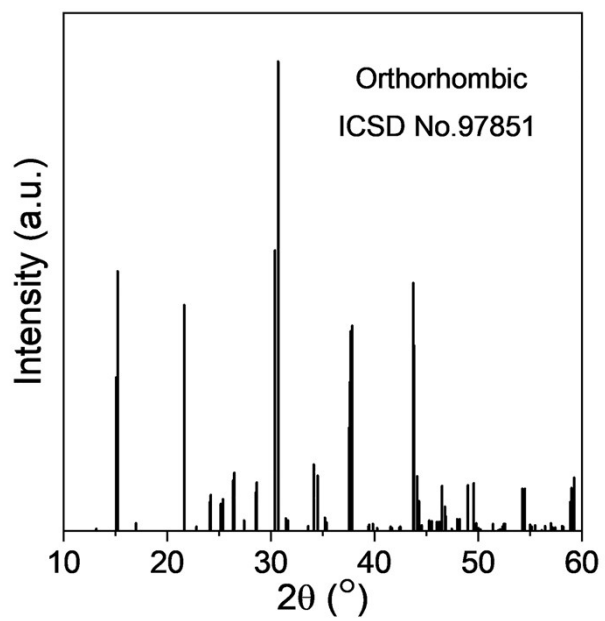


**Figure S1.** The XRD pattern of orthorhombic phase CsPbBr<sub>3</sub>.

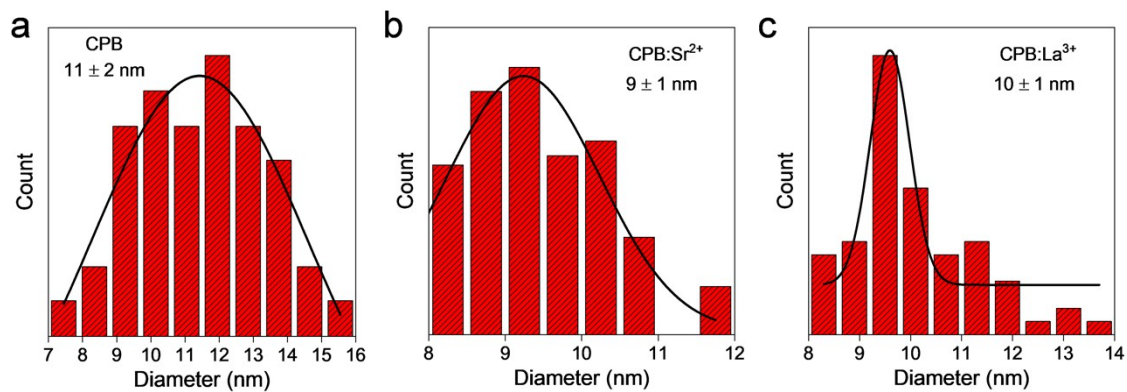


**Figure S2.** The size distribution statistics of (a) CsPbBr<sub>3</sub> NCs, (b) Sr<sup>2+</sup>-doped CsPbBr<sub>3</sub> NCs (1.50% Sr<sup>2+</sup>) and (c) La<sup>3+</sup>-doped CsPbBr<sub>3</sub> NCs (1.86% La<sup>3+</sup>).

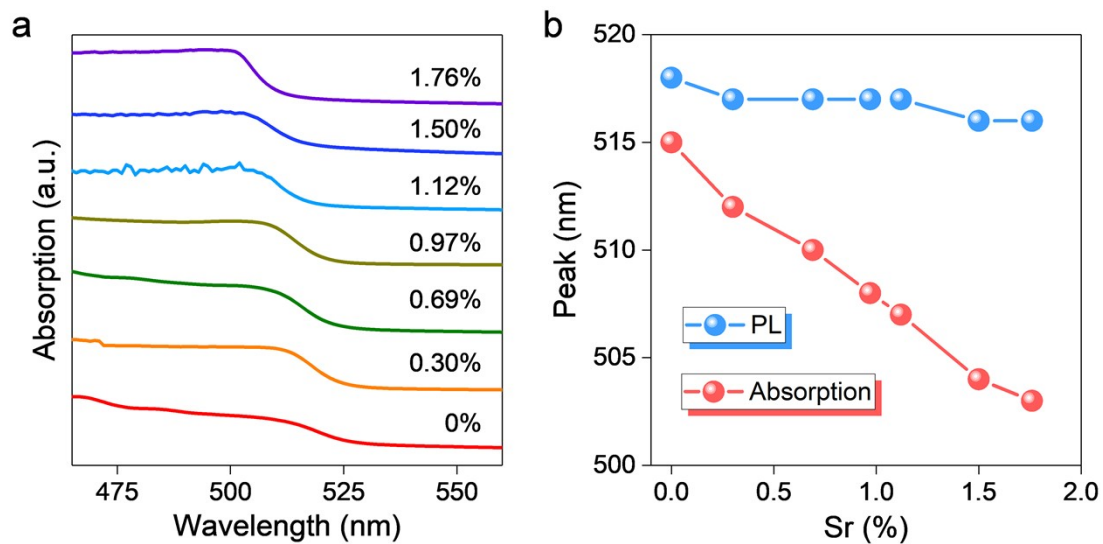


**Figure S3.** (a) UV-vis absorbance and (b) the position of absorption peak and PL peak of Sr<sup>2+</sup>-doped CsPbBr<sub>3</sub> NCs with different Sr<sup>2+</sup> ions concentrations.



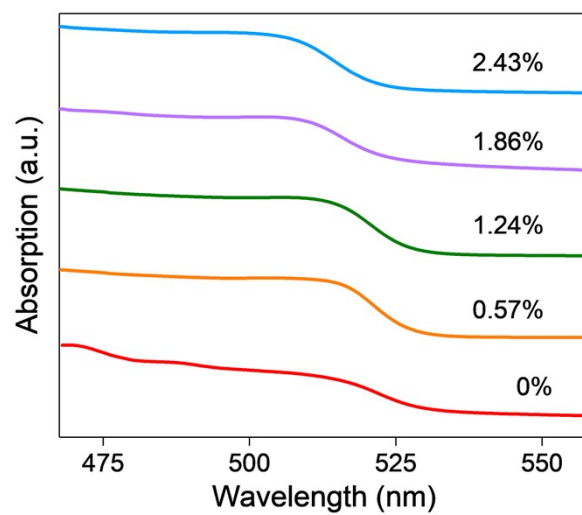


**Figure S4.** UV-vis absorption spectra of La<sup>3+</sup>-doped of CsPbBr<sub>3</sub> NCs with different La<sup>3+</sup> ions concentration.

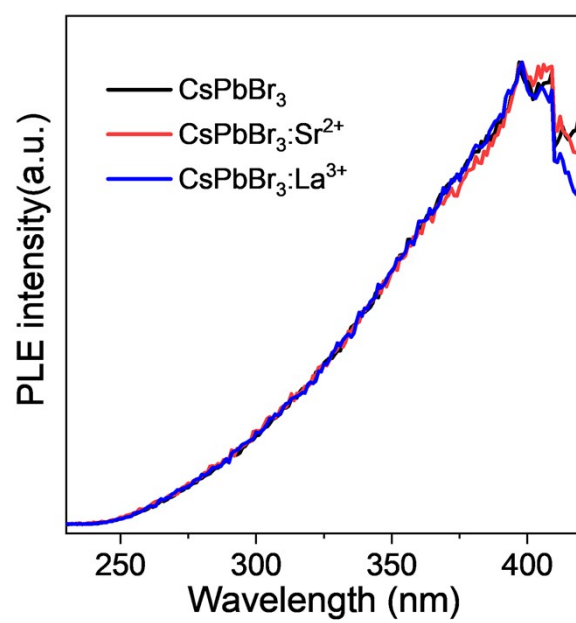


**Figure S5.** The excitation spectra of CsPbBr<sub>3</sub>, CsPbBr<sub>3</sub>:Sr<sup>2+</sup> and CsPbBr<sub>3</sub>:La<sup>3+</sup>.

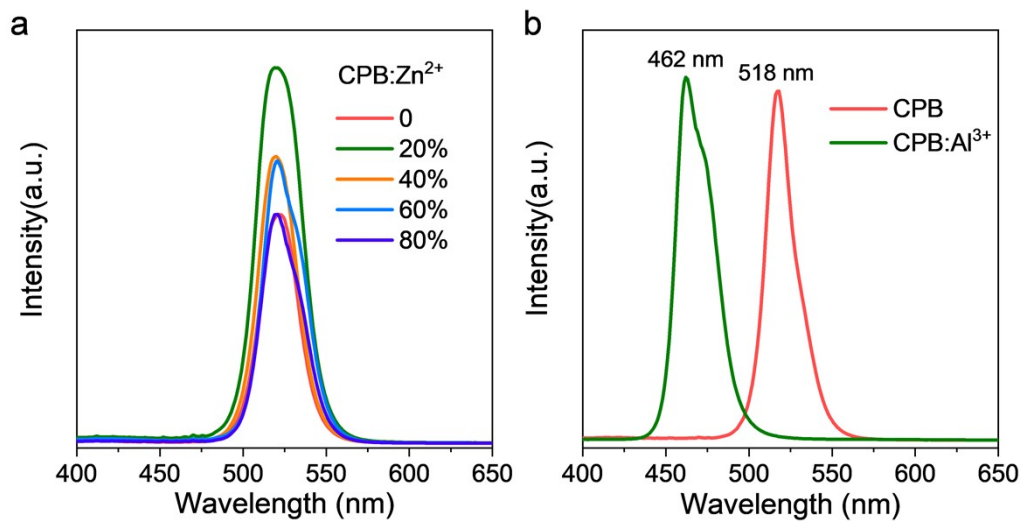


**Figure S6.** The PL spectra of (a) Zn<sup>2+</sup> doped CsPbBr<sub>3</sub> and (b) Al<sup>3+</sup> doped CsPbBr<sub>3</sub>.